

Supplementary Information for:

Crossover of Thermal Expansion from Positive to Negative by Removing the Excess Fluorines in Cubic ReO₃-type TiZrF_{7-x}

Cheng Yang,^{a,b} Yugang Zhang,^c Jianming Bai,^c Bingyan Qu,^d Peng Tong,^{*,a,b} Meng Wang,^a
Jianchao Lin,^a Ranran Zhang,^e Haiyun Tong,^{a,b} Ying Wu,^a Wenhai Song,^a and Yuping Sun^{*,a,e}

^a Key Laboratory of Materials Physics, Institute of Solid State Physics, Chinese Academy of Sciences, Hefei 230031, China

^b University of Science and Technology of China, Hefei 230026, China

^c National Synchrotron Light Source II, Brookhaven National Laboratory, Upton, NY 11973, United States

^d Laboratory of Amorphous Materials, School of Materials Science and Engineering, Hefei University of Technology, Hefei 230009, People's Republic of China

^e High Magnetic Field Laboratory, Chinese Academy of Sciences, Hefei 230031, China

***Corresponding Authors** *Email: tongpeng@issp.ac.cn (Peng Tong), *Email: ypsun@issp.ac.cn (Yuping Sun)

Table S1. Pyrohydrolysis determination of fluorine content

Sample	Initial weight (g)	Final weight (g)	Calculated F concentration	Theoretical F concentration
TZF6	0.10000	0.08054	44.84%	45.02%
TZF7	0.09999	0.07505	48.59%	48.88%
TiF ₃	0.10026	0.07678	54.10%	54.35%

The pyrohydrolysis process is similar to that reported by J. Peng et al. from Shanghai Institute of Applied Physics, Chinese Academy of Sciences (J. Fluor. Chem. 2017, 193, 106-112). This technology has been gradually applied to the determination of halogen in solid and waste treatment in the radioactive liquid with its development. According to their study on pyrohydrolysis of ZrF₄, a little amount of the sample will volatilize above 650°C. So first, the sample was heated to 600°C at water vapour atmosphere for 5h. Then the cooled production was transferred to pure oxygen (5N), followed by heating to 800°C for 20h to ensure absolute oxidation. Finally, the dark samples were transformed to white production. XRDs show the resulting productions are TiO₂ (for TiF₃) and (Zr,Ti)O₂ (namely, Ti doped ZrO₂) (for TZF6) as shown in Fig. S1. There is no impurity phase in both oxides. The initial weight of sample and the final weight of production were measured on a high-precision electronic balance. The resulted fluorine concentrations were calculated from the weight difference between metal fluorides and metal oxides. The fluorine concentrations for TZF6 and TZF7 are slightly less than those in nominal composition. Besides, the F concentration of TiF₃ measured is almost stoichiometric, which confirms the applicability of the method.

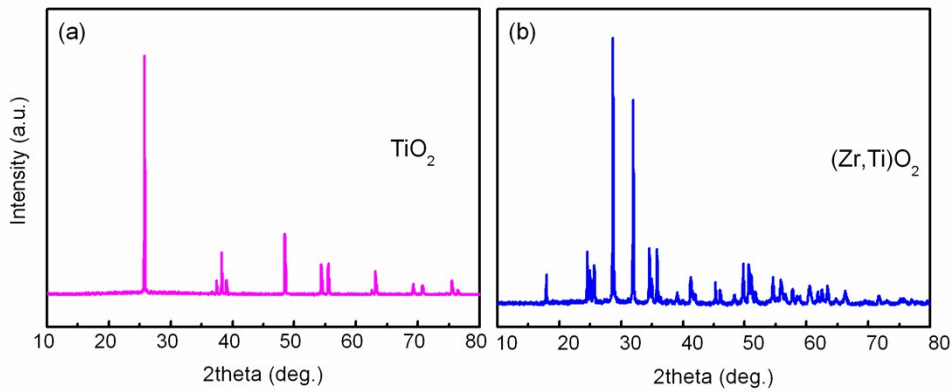


Fig. S1. XRD patterns of the resulted white production after pyrohydrolysis and oxidation of TiF_3 (a) and TZF6 (b).

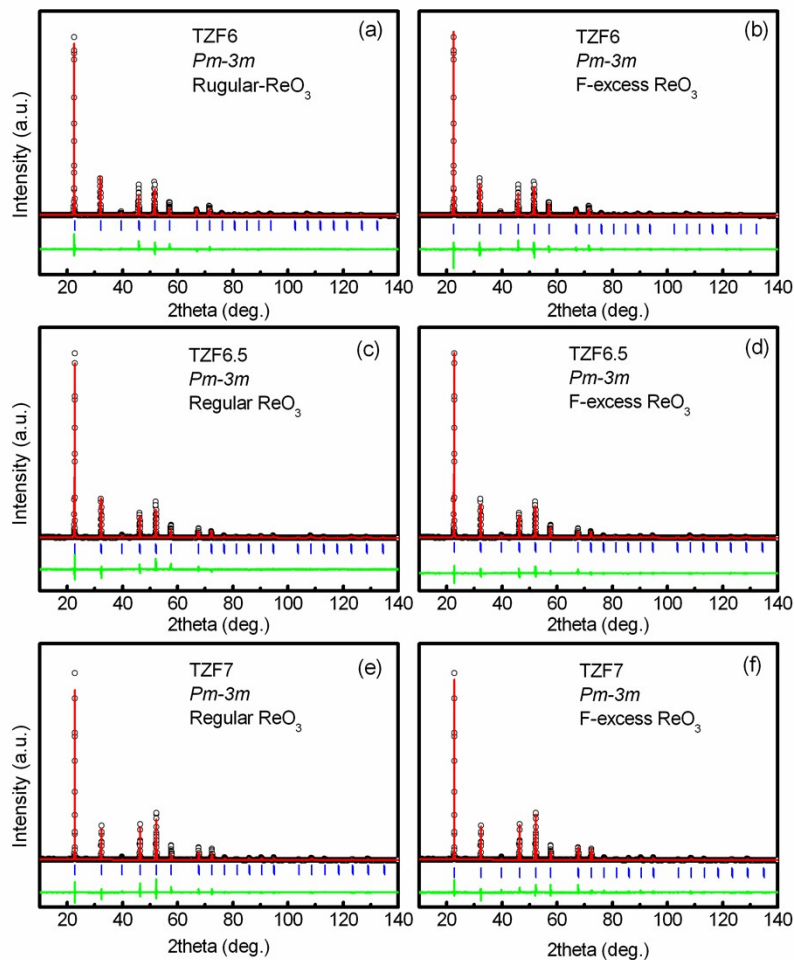


Fig. S2. Standard Rietveld refinements for XRD data of TiZrF_{7-x} , using the regular ReO_3 -type and anion-excess ReO_3 -type models, respectively. The fluorine concentrations are set as the values obtained from the experiment, without further fitting

in order to avoid results with no physical meaning. The refined results by F-excess ReO_3 model, which gives slightly better fitting, are shown in Table S2 below.

Table S2. Refined parameters of XRD data for TiZrF_{7-x} , using F-excess ReO_3 model

Sample	TZF7	TZF6.5	TZF6
Crystal system	cubic	cubic	cubic
Space group	<i>Pm-3m</i>	<i>Pm-3m</i>	<i>Pm-3m</i>
$a, b, c / \text{\AA}$	3.91155 (6)	3.92276 (5)	3.95002 (6)
R_p	4.372%	5.533%	7.605%
R_{wp}	6.523%	8.971%	10.260%
χ^2	1.301	1.826	2.177
U	0.22000	0.26000	0.31000
V	-0.04600	-0.04500	-0.03900
W	0.0086	0.0092	0.0079

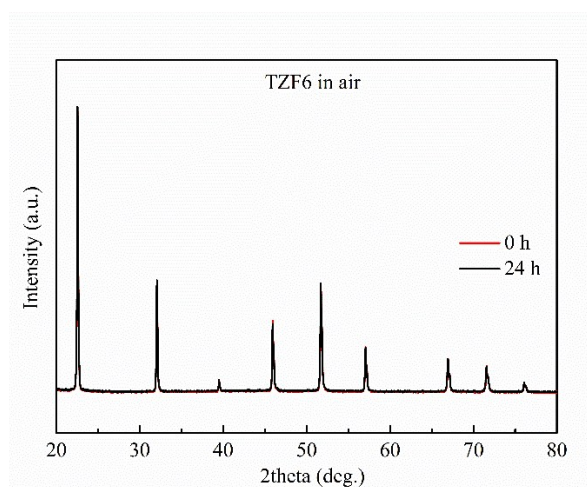


Fig. S3. The XRD patterns of the as-prepared TZF6 and the one exposed in the air for

24 hours exactly overlap with each other, indicating a good stability in air.

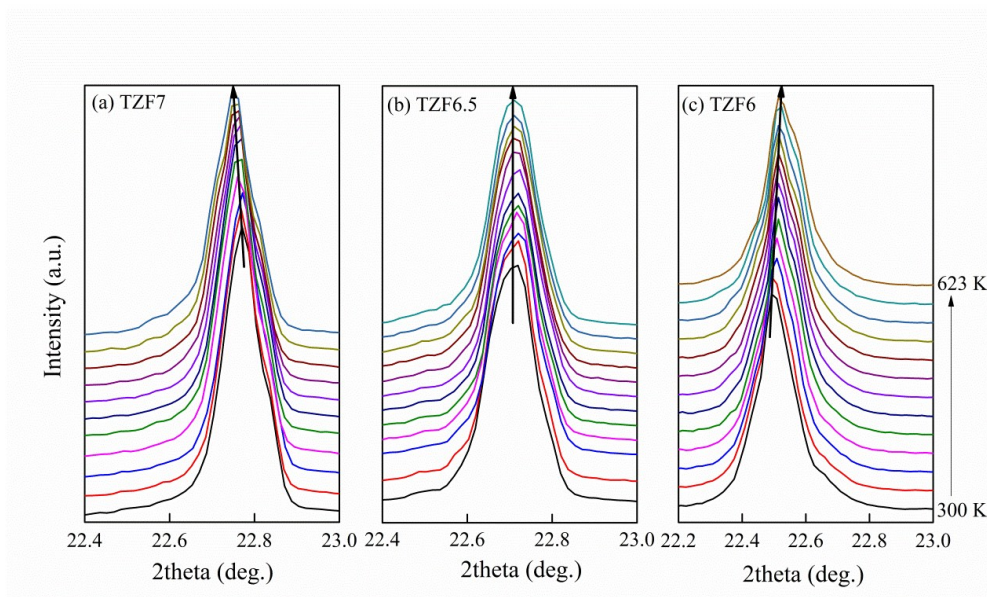


Fig. S4. The shift of (100) peak in XRD patterns of three samples with increasing temperature from 300 K to 623 K.

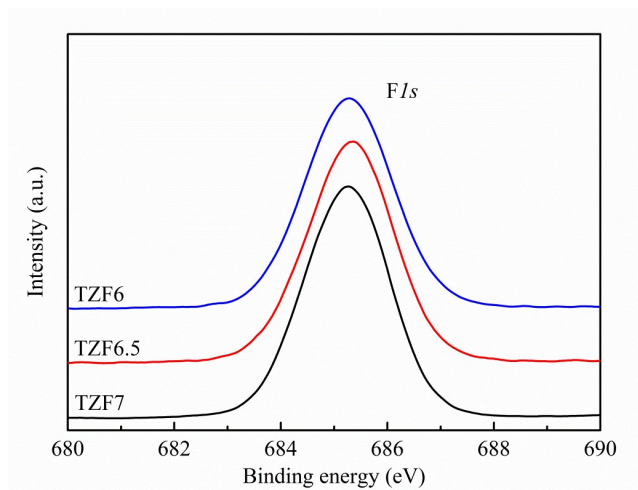


Fig. S5. The F 1s XPS peak for TZF7, TZF6.5 and TZF6.

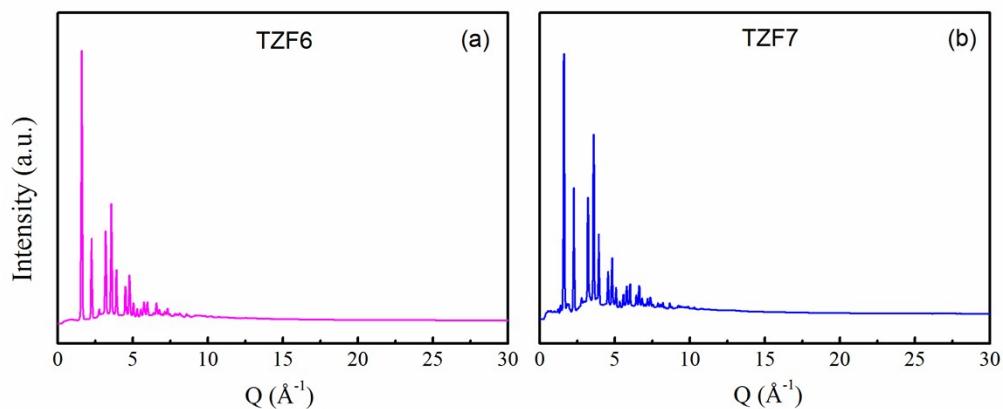


Fig. S6. The synchrotron powder diffraction patterns plotted as a function of Q : raw diffraction data for (a) TZF6 and (b) TZF7, with the monochromatic radiation wavelength of 0.1827 \AA .

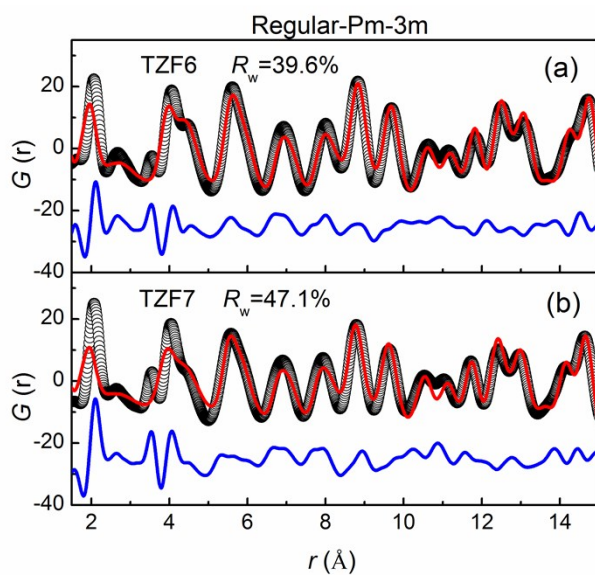


Fig. S7. Calculated $G(r)$ up to 15 \AA using the regular $Pm-3m$ model (the red line) together with the experimental $G(r)$ (circle) for TZF6 (a) and TZF7 (b) samples. The difference between calculated and experimental $G(r)$ s is shown at the bottom in each panel. The agreement factor of fitting, R_w , was listed in each panel.

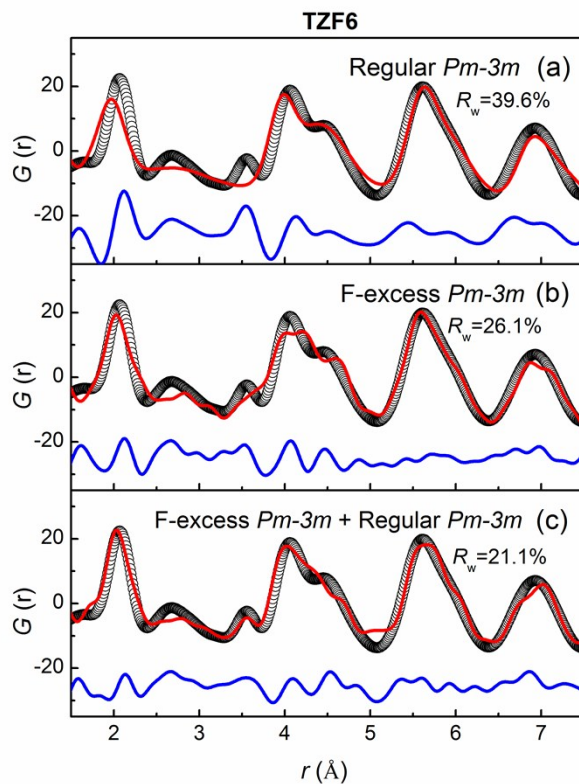


Fig. S8. Calculated $G(r)$ (the red line) up to 7.5 Å using the regular *Pm-3m* model (a), F-excess *Pm-3m* model (b) and a model combining both regular *Pm-3m* and F-excess *Pm-3m* (c) together with the experimental $G(r)$ (circle) for TZF6 sample. The difference between calculated and experimental $G(r)$ s is shown at the bottom in each panel. The agreement factor of fitting, R_w , was listed in each panel.

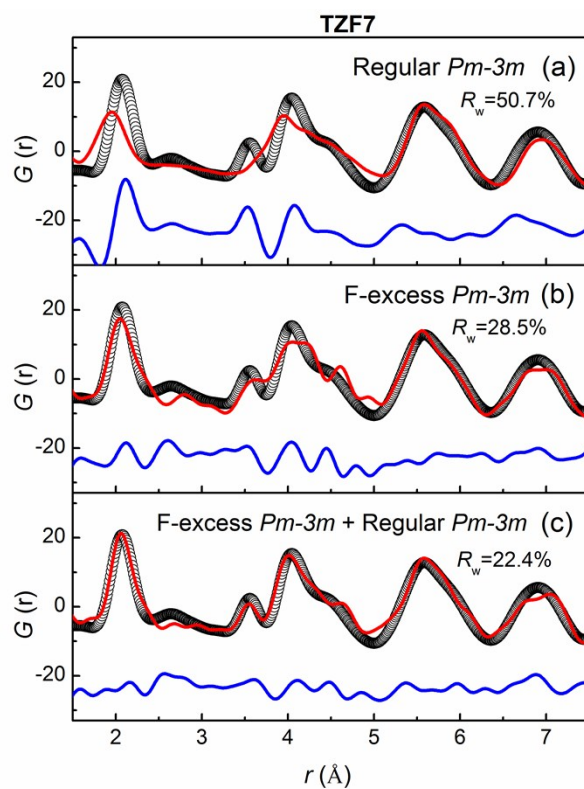


Fig. S9. Calculated $G(r)$ (the red line) up to 7.5 Å using the regular *Pm-3m* model (a), F-excess *Pm-3m* model (b) and a model combining both regular *Pm-3m* and F-excess *Pm-3m* (c) together with the experimental $G(r)$ (circle) for TZF7 sample. The difference between calculated and experimental $G(r)$ s is shown at the bottom in each panel. The agreement factor of fitting, R_w , was listed in each panel.